

# VISCOELASTIC MODEL FOR THERMOFORMING PROCESS OF THERMOPLASTIC COMPOSITE SHEETS

Mohammad Tahaye Abadi

*Aerospace Research Institute, Ministry of Science, Research and Technology,  
P. O. Box: 14665 – 834, Tehran, Iran, Email: [abadi@ari.ac.ir](mailto:abadi@ari.ac.ir)*

**SUMMARY:** An implicit finite element method is presented to analyze the thermoforming process of thermoplastic sheets reinforced with unidirectional continuous fibers. Unlike previous research works considering viscous or elastic behaviors for melted resin at the forming temperature, the reinforced laminates are regarded as an anisotropic viscoelastic material according to previous experimental studies. The transient reversible network theory is used to model the material behavior at the finite deformation. The kinematical constraints of material incompressibility and fiber inextensibility is considered in the finite element formulation. The present method is employed to analyze the picture-frame test of thermoplastic specimen reinforced with unidirectional fibers at forming temperature and the results are compared with the analytical solutions.

**KEYWORDS:** thermoforming, viscoelasticity, thermoplastic, Finite Element Analysis (FEA)

## INTRODUCTION

Thermoforming process is an effective fabrication method to produce final shapes in the thermoplastic composite laminates. To successfully investigate the formability of composite laminates and optimize the processing parameters in the forming process, an accurate and effective model and computational method are essential. The thermoforming of thermoplastic composite laminates is performed at the melting temperature of thermoplastic resin, in which the fibers obtain enough flexibility to move easily relative to each other to match the die geometry. By applying a mechanical contact force or a hydrostatic pressure, the laminates are moved into the die cavity to form the desired geometry. After completing deformation, the melted resin is cooled and solidified before the load removal. The high volume fraction of oriented fibers embedded in melted resin defines a highly anisotropic behavior and kinematical constraints that it complicates the analysis of forming process. Experimental studies have shown that continuous fibers define inextensible orientations in the reinforced thermoplastic laminates during forming process

[1] and the thermoplastic reinforced sheets behave like an incompressible material at the forming temperature [2].

In the present research work, an implicit finite element method is presented to analyze the thermoforming process of thermoplastic sheets reinforced with unidirectional continuous fibers. Unlike previous research works considering viscous [3-5] or elastic [6-7] behaviors for melted resin at the forming temperature, the reinforced laminates are regarded as an anisotropic viscoelastic material according to previous experimental studies [8-9]. The transient reversible network theory [10] is used to model anisotropic material behavior at the finite deformation. The kinematical constraints due to material incompressibility and fiber inextensibility are considered in the finite element formulation. The present method is employed to analyze the picture-frame experiment of thermoplastic specimen reinforced with unidirectional fibers at forming temperature and the results are compared with the exact solutions.

## CONTINUUM MODEL

To model the behavior of the thermoplastic laminates reinforced with unidirectional continuous fibers in the thermoforming process, the resin and fiber are macroscopically regarded as a single homogenized anisotropic material. A Lagrangian viewpoint is used to describe the material motion and the components of vectors and tensors are described in a fixed rectangular coordinate system. In the reference configuration of composite sheet, the position of a typical material particle is expressed with vector  $\mathbf{X}$  (components  $X_i$ ). In the deformed configuration at instance  $t$ , the particle moves to a position described with vector  $\mathbf{x}(\mathbf{x},t)$  (components  $x_i$ ) corresponding to the displacement vector  $\mathbf{u}(\mathbf{x},t)$  (components  $u_i$ ). The macroscopic state of the deformation is typically described using the deformation gradient, designated by  $\mathbf{F}$ , whose components are given by

$$F_{ik} = \frac{\partial x_i}{\partial X_k} \quad (1)$$

In the reference configuration, a unit vector  $\mathbf{a}_0$  (components  $a_{0k}$ ) is attributed along the tangent to the fiber direction. The fibers are regarded as material lines [11], so that the deformation gradient tensor describes the transformation between the initial and current fiber direction as

$$\mathbf{a}_{(t)} = \mathbf{F}_{(t)} \mathbf{a}_0 \quad (2)$$

According to the concept of transient reversible network [10], a viscoelastic behavior for the reinforced thermoplastic material is treated as a network of long chains connected to junctions. An active chain whose ends are connected to separate junction is analyzed as a hyperelastic model. Snapping of one end of an active link from a junction is tantamount to breaking the link. When a dangling chain captures one of the junctions in its neighborhood, a new adaptive link is created.

The melted thermoplastic resin of composite material is regarded as a network involving  $M$  different kinds of links. The network consists of  $Y_{m(0,0)}$  active links of  $m^{\text{th}}$  kind at the initial instant  $t = 0$ . The number of initial links existing at time  $t$  is designated by  $Y_{m(t,0)}$ . In addition to, the number of links arisen within the interval  $[\tau, \tau + d\tau]$  and existing at instant  $t$  can be given by  $(dY_{m(t,\tau)}/d\tau)d\tau$ . Hence, the total active links at instant  $t$  can be expressed as

$$Y_{(t,t)} = \sum_{m=1}^M \left( Y_{m(t,0)} + \int_0^t (\partial Y_{m(t,\tau)}/\partial \tau) d\tau \right) \quad (3)$$

In the present work, the composite materials are assumed to behave as a non aging viscoelastic media, in which the total number of active links remains unchanged and the rate of reformation is a constant value. In nonaging material, the number of broken links depends on the difference between the current instant and the instant of link formation. Hence, the functions of  $Y_{m(t,0)}$  and  $dY_{m(t,0)}/d\tau$  can be written as [12]

$$Y_{m(t,0)} = Y_{m(0,0)} \exp(-\Gamma_{m0}t) \quad , \quad \partial Y_{m(t,\tau)}/\partial \tau = Y_{m(0,0)} \Gamma_{m0} \exp[-\Gamma_{m0}(t-\tau)] \quad (4)$$

where  $\Gamma_{m0}$  is the reformation rate of active links. To calculate the response of the network at a specific instant, the strain energy stored in all existing links should be added together, i.e.

$$w_{(t,t)} = Y_{T(0,0)} \sum_{m=1}^M \left\{ [D_0 + D_m \exp(-\Gamma_{m0}t)] w_{m(t,0)} + \int_0^t D_m \Gamma_{m0} \exp[-\Gamma_{m0}(t-\tau)] w_{m(t,\tau)} d\tau \right\} \quad (5)$$

$Y_{T(0,0)}$  is the total of active links and  $D_m$  are constants defining the breakage and reformation functions. The strain energy stored in a hyperelastic materials reinforced with unidirectional continuous fibers is a scalar function of the right Cauchy-Green tensor ( $\mathbf{C} = \mathbf{F}^T \mathbf{F}$ ) and vector  $\mathbf{a}_{(\tau)}$  along the fibre direction at the instant of link formation. According to the invariant approach, the strain energy function can be represented as  $w_{m(I1,I2,I3,I4,I5)}$ , in which the invariants are given by

$$I_{1(t,\tau)} = \text{tr} \mathbf{C}_{(t,\tau)} \quad I_{2(t,\tau)} = \frac{1}{2} \left[ (\text{tr} \mathbf{C}_{(t,\tau)})^2 - \text{tr} \mathbf{C}_{(t,\tau)}^2 \right] \quad I_3 = \det \mathbf{C}_{(t,\tau)} \quad (6)$$

$$I_{4(t,\tau)} = \mathbf{A}_{(\tau)} : \mathbf{C}_{(t,\tau)} \quad I_5 = \mathbf{A}_{(\tau)} : \mathbf{C}_{(t,\tau)}^2$$

where  $\mathbf{A}_{(\tau)}$  is a symmetric second order tensor with the components of  $A_{ij(\tau)} = a_{i(\tau)} a_{j(\tau)}$ . The strain energy of a hyperelastic materials reinforced with unidirectional fibers can be given by

$$w_m = \frac{1}{2} \frac{\beta_{m1}}{Y_{T(0,0)}} (I_1 - 3) + \left( \frac{1}{4} \frac{\beta_{m3}}{Y_{T(0,0)}} (\ln I_3)^2 - \frac{1}{2} \frac{\beta_{m1}}{Y_{T(0,0)}} \ln I_3 \right) \quad (7)$$

$$+ \frac{1}{4} \frac{\beta_{m4}}{Y_{T(0,0)}} (I_4 - 1)^2 - \frac{\beta_{m5}}{Y_{T(0,0)}} (I_4 - 1) + \frac{1}{2} \frac{\beta_{m5}}{Y_{T(0,0)}} (I_5 - 1)$$

where  $\beta_{mi}$  are  $m^{\text{th}}$  link constants. In order to enforce the incompressibility and inextensibility constrains with negligible errors, the constants  $\beta_{m3}$  and  $\beta_{m4}$  must be large enough compare to  $\beta_{m1}$  and  $\beta_{m5}$ , respectively. Assuming constants of active links are the

same ( $\beta_{mi} = \beta_{0i}$ ) and taking derivative of strain energy respect to the right Cauchy-Green tensor yield the second Piola-Kirchhoff stress tensor as follows

$$\mathbf{S}_{(t)} = g_{(t)} \left\{ \mu_1^0 \mathbf{I} + (2\mu_3^0 \ln J_{(t)} - \mu_1^0) \mathbf{C}_{(t)}^{-1} + [\mu_4^0 (I_{4(t)} - 1) - 2\mu_5^0] \mathbf{A}_o + \mu_5^0 (\mathbf{C}_{(t)} \mathbf{A}_o + \mathbf{A}_o \mathbf{C}_{(t)}) \right\} + \int_0^t G_{(t-\tau)} \left\{ \begin{aligned} & \left[ \mu_1^0 \mathbf{C}_{(\tau)}^{-1} + (2\mu_3^0 \ln J_{(t,\tau)} - \mu_1^0) \mathbf{C}_{(t)}^{-1} + [\mu_4^0 (I_{4(t,\tau)} - 1) - 2\mu_5^0] \mathbf{A}_o \right] \\ & + \mu_5^0 (\mathbf{C}_{(\tau)}^{-1} \mathbf{C}_{(t)} \mathbf{A}_o + \mathbf{A}_o \mathbf{C}_{(t)} \mathbf{C}_{(\tau)}^{-1}) \end{aligned} \right\} d\tau \quad (8)$$

Where  $g_{(t)}$  and  $G_{(t-\tau)}$  are functions defined by

$$g_{(t)} = D_0 + \sum_{m=1}^M D_m \exp(-\Gamma_0^m t) \quad G_{(t-\tau)} = D_m \Gamma_0^m \exp[-\Gamma_0^m (t - \tau)] \quad (9)$$

## FINITE ELEMENT FORMULATIONS

A Lagrangian finite element formulation is developed to handle complicated boundaries and follow the material points in order to model the large deformation of the history dependent behavior of composite materials in the forming process. In the finite element analysis, the reference material geometry is subdivided into a suitable number of elements having the initial volume of  $\Omega_{0e}$ . The displacement vector of node  $I$  at instant  $t$  is denoted by  $\mathbf{u}_{I(t)}$  (components  $u_{Ii}$ ). Using appropriate interpolation functions, denoted by  $N_{I(x)}$ , the displacement vectors are given by

$$\mathbf{u}_{(x,t)} = N_{I(x)} \mathbf{u}_{I(t)} \quad (10)$$

To discretize the equilibrium equation in the finite element analysis, a weak form, often called the variational form, is needed. For this purpose, a test function using the nodal virtual displacement  $\delta \mathbf{u}_I$  is defined that satisfies all boundary conditions. The weak form is obtained by taking the product of the equilibrium equation with the test function and integrating over the element volume, which gives

$$\delta \mathbf{u}_I^T (\mathbf{f}_I^{\text{int}} - \mathbf{f}_I^{\text{ext}}) = 0. \quad (11)$$

where  $\mathbf{f}_I^{\text{int}}$  and  $\mathbf{f}_I^{\text{ext}}$  denote, respectively, the internal and external forces applied at node  $I$  defined by:

$$\mathbf{f}_I^{\text{int}} = \int_{\Omega_{0e}} \mathbf{F}_{(t)} \mathbf{S}_{(t)} \mathbf{L}_I^0 d\Omega_0 \quad (12)$$

$$\mathbf{f}_I^{\text{ext}} = \int_{\Omega_{0e}} N_I \rho_0 \mathbf{b} d\Omega_0 + \int_{\Gamma_{0\sigma}} N_I \mathbf{q}_0 d\Gamma_0 \quad (13)$$

Where  $\mathbf{q}_0$  is the traction force applied on the reference exterior surfaces denoted by  $\Gamma_{0\sigma}$ ,  $\rho_0$  is initial material density,  $\mathbf{b}$  is the body force, and  $\mathbf{L}_I^0$  is a vector including the first order derivative of shape function respect to the reference material position given by

$$\mathbf{L}_I^0 = \left[ \frac{\partial N_I}{\partial X_1} \quad \frac{\partial N_I}{\partial X_2} \quad \frac{\partial N_I}{\partial X_3} \right]^T \quad (14)$$

Since inertia force has negligible effects on the typical forming process, it was eliminated in the linear momentum equation. The finite element formulation depends nonlinearly on the nodal displacement vectors because the stress tensor is a nonlinear function of the current material geometry. In the present work, a Newton-Raphson method is used to calculate the deformed geometry. Considering Taylor expansion of Eq. (11) and dropping terms of higher order than linear displacement increment result in

$$\delta \mathbf{u}_I (\mathbf{K}_{IJ}^{\text{int}} - \mathbf{K}_{IJ}^{\text{ext}}) \Delta \mathbf{u}_J = -\mathbf{f}_I^{\text{int}} + \mathbf{f}_I^{\text{ext}} \quad (15)$$

where  $\mathbf{K}_{IJ}^{\text{int}}$  and  $\mathbf{K}_{IJ}^{\text{ext}}$  are the components of internal and external Jacobean matrices defined by

$$\mathbf{K}_{IJ}^{\text{int}} = \frac{\partial \mathbf{f}_I^{\text{int}}}{\partial \mathbf{u}_J}, \quad \mathbf{K}_{IJ}^{\text{ext}} = \frac{\partial \mathbf{f}_I^{\text{ext}}}{\partial \mathbf{u}_J} \quad (16)$$

The external Jacobean matrix is defined for the follower loads which their values and directions depend on the configuration of the body. Taking the nodal displacement derivative of internal force defined in Eq. (12) yields the internal Jacobean matrix

$$\mathbf{K}_{IJ}^{\text{int}} = \mathbf{K}_{IJ}^{\text{geo}} + \mathbf{K}_{IJ}^{\text{mat}} \quad (17)$$

where  $\mathbf{K}_{IJ}^{\text{geo}}$  and  $\mathbf{K}_{IJ}^{\text{mat}}$  are the matrices and defined by

$$\mathbf{K}_{IJ}^{\text{geo}} = \int_{\Omega_{0e}} (\mathbf{L}_I^{0T} \mathbf{S}_{(t)} \mathbf{L}_J^0) \mathbf{1} d\Omega_0 \quad (18)$$

## RESULTS AND DISCUSSION

The validity of the developed finite element formulation was investigated through analyzing the picture-frame experiment which is used to study the rheological behavior of thermoplastic materials reinforced with unidirectional fibers or woven fabrics at the forming temperature.

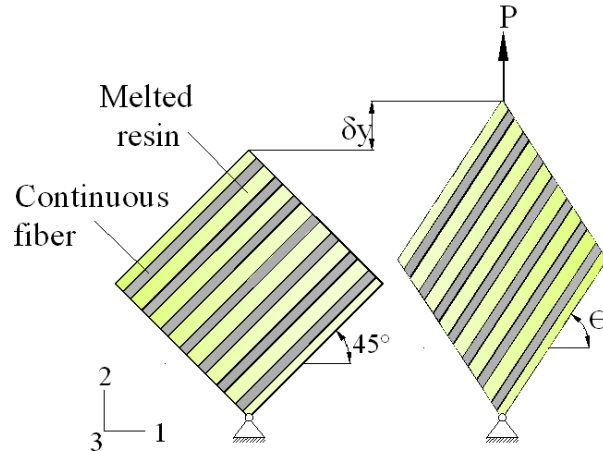


Fig. 1 Schematic of picture-frame experiment of unidirectional reinforced thermoplastic specimen.

$$\begin{aligned}
\mathbf{K}_{IJ}^{mat} = & \int_{\Omega_0} \left( \mathbf{g}_{(t)} \right) \left\{ \begin{aligned} & + 2\lambda_0^0 \mathbf{L}_I \mathbf{L}_J^T - \\ & (2\lambda_0^0 \ln J_{(t)} - \mu_1^0 - 2\mu_2^0) \left[ (\mathbf{L}_I^T \mathbf{L}_J) \mathbf{I} + \mathbf{L}_J \mathbf{L}_I^T \right] + \\ & + 2\mu_4^0 \mathbf{F}_{(t)} \mathbf{A}_0 \mathbf{L}_I^0 \mathbf{L}_J^{0T} \mathbf{A}_0 \mathbf{F}_{(t)}^T \\ & + \mu_5^0 \left[ \mathbf{F}_{(t)} \mathbf{L}_J^0 \mathbf{L}_I^{0T} \mathbf{A}_0 \mathbf{F}_{(t)}^T + (\mathbf{L}_I^{0T} \mathbf{A}_0 \mathbf{L}_J^0) \mathbf{F}_{(t)} \mathbf{F}_{(t)}^T \right] \\ & + \mu_5^0 \left[ \mathbf{F}_{(t)} \mathbf{A}_0 \mathbf{L}_J^0 \mathbf{L}_I^{0T} \mathbf{F}_{(t)}^T + (\mathbf{L}_I^{0T} \mathbf{L}_J^0) \mathbf{F}_{(t)} \mathbf{A}_0 \mathbf{F}_{(t)}^T \right] \end{aligned} \right\} d\Omega_0 \\
+ & \int_{\Omega_0} \int_0^t G_{(t,\tau)} \left\{ \begin{aligned} & 2\lambda_0^0 \mathbf{L}_I \mathbf{L}_J^T - \\ & (2\lambda_0^0 \ln J_{(t,\tau)} - \mu_1^0) \left[ (\mathbf{L}_I^T \mathbf{L}_J^0) \mathbf{I} + \mathbf{L}_J \mathbf{L}_I^T \right] + \\ & + 2\mu_4^0 \mathbf{F}_{(t)} \mathbf{A}_0 \mathbf{L}_I^0 \mathbf{L}_J^{0T} \mathbf{A}_0 \mathbf{F}_{(t)}^T + \\ & + \mu_5^0 \left[ \mathbf{F}_{(t)} \mathbf{C}_{(\tau)}^{-1} \mathbf{L}_J^0 \mathbf{L}_I^{0T} \mathbf{A}_0 \mathbf{F}_{(t)}^T + (\mathbf{L}_I^{0T} \mathbf{A}_0 \mathbf{L}_J^0) \mathbf{F}_{(t)} \mathbf{C}_{(\tau)}^{-1} \mathbf{F}_{(t)}^T + \right] \\ & + \mu_5^0 \left[ \mathbf{F}_{(t)} \mathbf{A}_0 \mathbf{L}_J^0 \mathbf{L}_I^{0T} \mathbf{C}_{(\tau)}^{-1} \mathbf{F}_{(t)}^T + (\mathbf{L}_I^{0T} \mathbf{C}_{(\tau)}^{-1} \mathbf{L}_J^0) \mathbf{F}_{(t)} \mathbf{A}_0 \mathbf{F}_{(t)}^T \right] \end{aligned} \right\} d\tau d\Omega_0
\end{aligned} \tag{19}$$

A schematic of picture frame experiment is shown in Fig. 1, in which an initially square specimen attached to a four-bar linkage is subjected to a stretching force along a diagonal line that deforms it to a rhombus. The fibers are parallel to the sides of specimen and the fiber angle changes as the deformation process proceeds.

An 8 node bi-quadratic quadrilateral element was used to analyze the picture-frame experiment. The reinforced sample with length  $L$  was deformed vertically by stretching the vertical diagonal up to  $2L/15$  with a constant velocity and the required force is calculated during deformation process. Since the lateral surfaces of the sheet are free from traction and the sheet has small thickness, a state of plane stress is considered. The material constant was set to  $\beta_{m5} / \beta_{m0} = 1$  and  $\beta_{m4} / \beta_{m5} = 10^5$ . Table 1 shows the parameters considered to define the breakage function and reformation rate of active links in the viscoelastic model.

Table 1 Parameters defining the number of active links in the viscoelastic model

$\Gamma_{m0}$	$D_m$
0.01	0.05
0.1	0.25
1	0.4
10	0.3

In order to define the appropriate increment number required to analyze the total deformation process, the calculated forced was compared with exact solution in Fig. 2. In order to calculate the internal nodal force and Jacobean matrix defined in the previous section, the integral form of the constitutive equation was evaluated by trapezoid approximation. Hence, a considerable error is observed for a single increment. As shown in Fig. 2, a reasonable accuracy can be obtained for more than ten increments.

The finite element results are compared with exact solution in Fig. 3, in which the variation of forming force during deformation process are shown in different velocities. Although the specimens were stretched up to the same value in different velocities, the forming force decreases for slow deformation rate as observed in the experimental results [13]. Since there is enough time to snap more active links for a slow deformation rate, the calculated forming force decreases depending on the parameters used in the viscoelastic model. As shown in Fig. 3, there is a good agreement between the exact solution and the finite element results computed in ten increments. Unlike the theory of *ideal fiber reinforced fluids*, in which each composite laminate is modeled as a transversely isotropic Newtonian fluid [3], the calculated forming force depends nonlinearly on the rate of deformation in the present finite element formulation. Hence, the present method can be used to model rate of deformation effects in the sheet forming process of the reinforced thermoplastic materials at the elevated temperature.

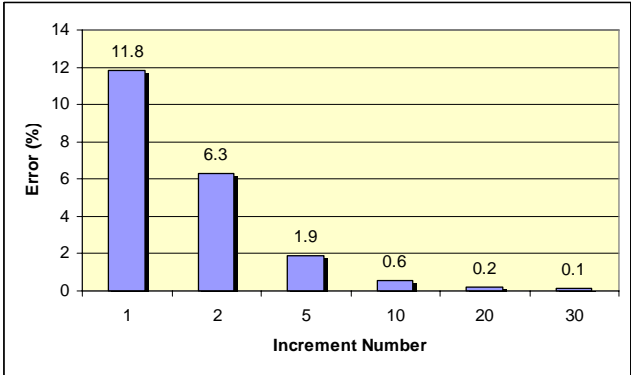


Fig. 2 Error of finite element results for different increment numbers.

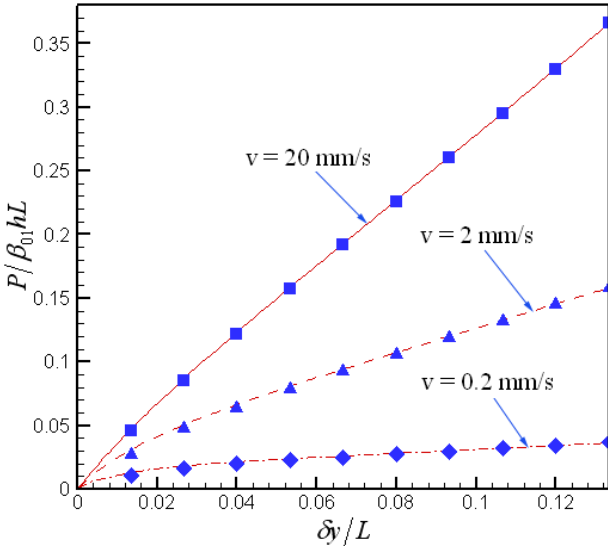


Fig. 3 Comparison of exact solution and finite element results calculating picture frame force for different deformation rates.

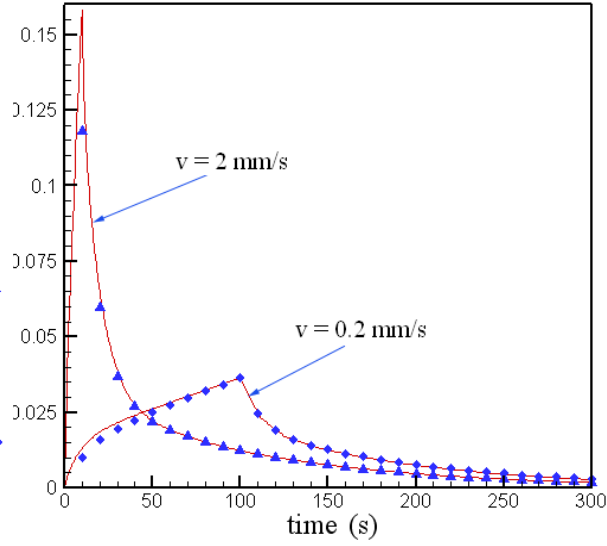


Fig. 4 Relaxation force in the picture frame test.

In the picture frame experiment, the force required to maintain a specific deformation is also measured to investigate the stress relaxation in the composite sample. In the reinforced viscous model considered in the previous research works, the calculated forming force drops to a zero value as soon as the deformation stops. The finite element formulation of viscoelastic model used in the present works yields a convenient method to analyze the stress relaxation phenomenon. Fig. 4 shows the history of required force to produce and maintain a prescribed deformation in the picture-frame experiment. The diagonal stretch of  $2L/15$  is applied at the two different velocities of 2 mm/s and 0.2 mm/s and it was held for a sufficiently long time. As soon as the deformation stops, the force relaxes according to the rate of breakage of active link in the viscoelastic model. Therefore, the relaxation force measured in the picture frame experiment can be used to determine the parameters defined in the number of active chains considered in the transient reversible theory.

## CONCLUSIONS

The present finite element formulations provide an effective procedure to analyze the large deformation of the highly anisotropic behavior and kinematical constraints defined in thermoplastic laminates reinforced with unidirectional continuous fibers at forming temperature. The viscoelastic model developed based on the reversible network theory provides a convenient method to consider the history of deformation in the material response. The present finite element method of viscoelastic model provides a convenient procedure to model the rate of deformation effects as well as the stress relaxation phenomenon observed in the sheet forming process of the reinforced thermoplastic materials at the elevated temperature. The finite element analysis shows that the picture-frame experiments can be used to determine the parameters of breakage and reformation function of the active links considered in the viscoelastic model.

## REFERENCES

1. M. Tahaye Abadi, H.R. Daghyani, Sh. Fariborz, "Experimental Wrinkling Analysis in Stamp Forming of Continuous Fibre Reinforced Thermoplastic Sheets, *Proc. of Tehran International Congress in Manufacturing Engineering (TICME)*, Tehran, Iran, 2005.
2. S.G. Advani, T.S. Creasy, S.F. Shuler, "Rheology of Long Fibre-Reinforced Composites in Sheet Forming", In: D. Bhattacharyya, editor, *Composite Sheet Material, Composite Material Series*, Vol. 11, Elsevier Pub., 1997.
3. C.M.O'Brádaigh, G.B. McGuinness, S.P. McEntee, "Implicit Finite Element Modelling of Composites Sheet Forming Processes", In: D. Bhattacharyya, editor, *Composite Sheet Material, Composite Material Series, Vol. 11, Elsevier Pub.*, 1997.
4. T.C. Lim, S. Ramakrishna, "Modelling of Composite Sheet Forming: a Review", *Composites Part A*, 33, 2002, pp. 515-537.



5. M. T. Abadi, H. R. Daghyani, S.H. Fariborz, "Finite Element Analysis of Thermoplastic Composite Plates in Forming Temperature", *Composite Science and Technology*, 66, 2006, pp. 306-313.
6. W. R. Yu, M. Zampaloni, F. Pourboghrat, K. Chung, T. J. Kang, "Sheet Hydroforming of Woven FRT Composites: Non-Orthogonal Constitutive Equation Considering Shear Stiffness and Undulation of Woven Structure", *Composite Structures*, Vol. 61, 2003, pp. 353-362.
7. J. Cao, P. Xue, X. Peng, N. Krishnan, "An Approach in Modelling the Temperature Effect in Thermo-Stamping of Woven Composites", *Composite Structures*, Vol. 61, 2003, pp. 413-420.
8. G. B. McGuinness, C. M. Ó Brádaigh, "Development of Rheological Models for Forming Flows and Picture-Frame Shear Testing of Fabric Reinforced Thermoplastic Sheets", *Journal of Non-Newtonian Fluid Mechanics*, Vol. 73, 1997, pp. 1-28.
9. Martin TA, Bahattacharyya D, Collins IF, "Bending of Continuous Fibre- Reinforced Thermoplastic Sheets", *Composites Manufacturing*, 1998; 6(3-4): 177-187.
10. Tanaka, F. and Edwards, S. F., "Viscoelastic Properties of Physically Cross-Linked Networks. Transient Network Theory", *Macromolecules*, 1995, 25: 1516-1523.
- A. J. M. Spencer, "Theory of Fabric-Reinforced Viscose Fluid", *Composite Part A*, Vol. 31, 2000, pp.1311-1321.
11. Drozdov, A. D., "Mechanics of Viscoelastic Solids", *John Wiley & Sons*, 1998.
12. G.B. McGuinness and C.M. Ó Brádaigh, "Characterisation of Thermoplastic Composite Melts in Rhombus-Shear: the Picture-Frame Experiment", *Composites Part A*, 29, 1998, pp. 115-132.